

Application of Models to Design Studies of Concrete Airfield Pavements

F. M. MELLINGER, *Director*, and

P. F. CARLTON, *Chief of Research Analysis Branch,*
Ohio River Division Laboratories, Corps of Engineers, U. S. Army

This paper reports one phase of the Corps of Engineers Rigid Pavement Investigational Program conducted in connection with the design and construction of concrete airfield pavements. Previous papers outlining the scope of the program have been presented in the Highway Research Board Proceedings of 1944, 1948, 1950 and 1951. (See References 1-4). The model techniques described are the result of development and application over the past 12 years, during which time they have been used to correlate the results obtained from other phases of the investigational program. Specifically the paper deals with the details attendant to the design and construction of typical models, as well as a description of the test equipment and procedures used. Model measurements are related to the prototype and to the applicable theory. Summaries of test results are presented from studies of the effect of high contact pressures on rigid pavements and the relative load distribution characteristics of selected multiple wheel gear configurations. Curves relating pavement thickness requirements to tire inflation pressure are shown for 25 and 50 Kip loadings on a single wheel, and for 100 Kip loading on dual wheels spaced 37.5 inches center to center. Relative critical stresses are shown for dual wheel, twin-tandem, and quadricycle gear for equal wheel loads. Curves are included for translating multiple wheel loadings into an equivalent single wheel load.

● TO employ models successfully for a study such as this, two conditions must be fulfilled. First, the models should simulate as closely as possible the assumptions necessary in a theoretical solution of the problem to be investigated, if such a solution exists; and second, relationships must be established for relating the physical characteristics of the model to those of the prototype.

Fortunately, there are two theoretical approaches reasonably well developed for the analysis of stresses resulting from loadings on rigid concrete airfield pavements. These are the solutions for stresses and deflections at the edge and interior of a pavement slab as developed by the late H. M. Westergaard (5), and those more recently developed by Dr. Gerald Pickett (6). The basic difference between these two theories is that the Westergaard development assumes a constant modulus of subgrade support, as is represented by the displacement of a dense liquid; while Pickett's development is based on the assumption that the subgrade or supporting medium

acts as an elastic solid. Both assumptions can be used in varying degree in evaluating the data obtained from the models. The evaluation of these particular characteristics of the model requires considerable experience, as is true in actual practice. Since the Westergaard Theory is used more extensively in rigid pavement design, it has been used predominately in the correlation of the model tests with the theory.

In designing the model, the initial consideration must be the physical constants for the materials simulating the prototype subgrade and pavement slab. These constants are:

E_m = modulus of elasticity of the model slab

μ_m = Poisson's ratio of the model slab

k_m = modulus of subgrade reaction of the model subgrade

G_m = modulus of elasticity in shear of the model subgrade

The value of k_m applies to Westergaard's Dense Liquid Theory, while G_m applies to Pickett's Elastic Solid Theory.

For the studies described in this paper, the control of the model similitude to the prototype

follows the assumptions and resultant theory developed by Westergaard. This involves the establishment of one basic relationship for dimensional control, which is that:

$$\frac{l}{r} = \frac{l_m}{r_m} \quad (1)$$

where l is the radius of relative stiffness, defined as:

$$l = \left[\frac{Eh^3}{12(1 - \mu^2)k} \right]^{1/4}$$

h = pavement thickness

r = radius of a circular loaded area, or circular tire print area.

For the notation used in this paper, quantities designated by the subscript m refer to the model and quantities without the subscript m refer to the prototype.

The linear horizontal dimensions of the model slab are kept sufficiently large so that the assumptions of infinite and semi-infinite extent for interior and edge loading, respectively, are satisfied. Similarly, the horizontal and vertical dimensions of the model subgrade are selected to give the effect of an infinite medium.

Thus far, only a proportional dimensional relationship based on the constants of the construction materials is established. In this particular study, it remains only to establish a relationship between the model and the prototype for stresses and loadings. In this instance, resort is made to Westergaard's equations for interior and edge loading as given in Reference 5. For a circular loaded area, the following relationships can be developed for interior and edge loading:

Interior Loading:

$$\frac{\sigma}{\sigma_m} = \frac{Ph_m^2(1 + \mu)}{P_m h^2(1 + \mu_m)} \quad (2)$$

Edge Loading:

$$\frac{\sigma}{\sigma_m} = \frac{Ph_m^2(1 + \mu)(3 + \mu_m)}{P_m h^2(1 + \mu_m)(3 + \mu)} \quad (3)$$

where σ = maximum unit stress in lbs/in.²
 P = total load in lbs.

MODEL DESIGN

The model slabs are constructed of Hydrostone gypsum cement mortar and are formed accurately between two glass plates to a thickness h_m . Due to a slight expansion of the Hydrostone during the set, it is not possible to predict h_m within accuracies greater than 0.002 to 0.004 inch. When properly cured, this material has an $E_m = 3 \times 10^6$ psi, $\mu_m = 0.25$, and a flexural strength of approximately 2500 psi. The linear horizontal dimensions of the slabs are 15 x 15 inches square, which satisfy the assumption that the slabs will exhibit the characteristics of an infinite slab for both interior and edge loading.

During the testing, the model slab is supported by and is in continuous contact with the surface of a block of natural rubber 24 inches square and 12 inches deep. This arrangement is shown in Figure 1. The rubber block is rigidly supported by a concrete pedestal and the four sides of the block are restrained by a rigid casing. Measured values of k_m are 35 lbs/in.³ for interior loading and 65 lbs/in.³ for edge loading. For correlating test data with the Elastic Solid Theory, the value of $(G_m/1 - \mu_m)$ for the rubber is 111 lbs/in.². As can be seen from Figure 1, the model slab is uniformly loaded with a layer of small lead cubes. This load is in addition to that representing the prototype wheel load and serves to provide a better simulation of mass with respect to the prototype slab.

The load imposed by the prototype wheel is simulated by loading the model slab through a circular footprint. The footprint consists of a circular rubber pad cemented to a conforming rigid die. A load, P_m , is applied through this footprint by means of a reaction beam as shown in Figure 1. The choice of P_m is somewhat arbitrary and is restricted by the requirements that the maximum stresses not exceed the elastic limit of the Hydrostone, that the experimental error be kept to a minimum percentage by utilizing a wide range of stresses, and that an adequate factor of safety be maintained against accidental failure of the slab during the testing.

Model strains are measured by means of type A-7, SR-4 bonded resistance wire strain gages. These gages have an active length of 0.25 inch and may be statically strained up to 2 percent elongation without being damaged. Strains, in micro-inches, are read directly

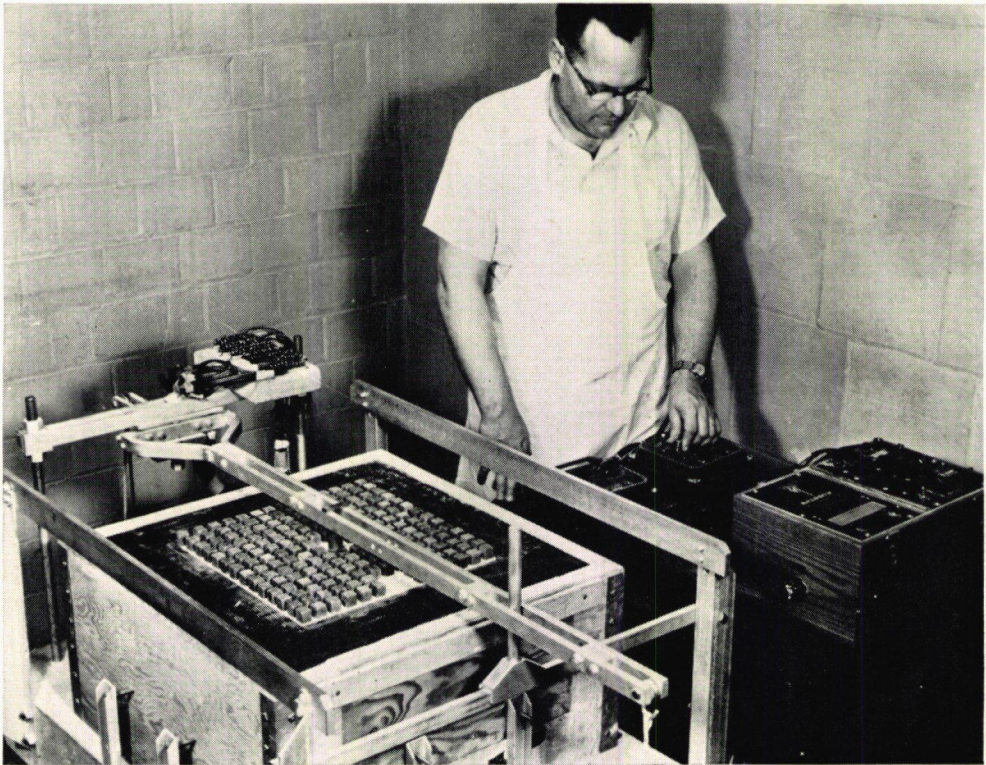


Figure 1

using a Baldwin SR-4 control box equipped with a spotlight type galvanometer. For interior loading, the maximum strains are obtained from a gage placed directly beneath the center of the loaded area and oriented so that the strain is measured in a radial direction with respect to the load. For edge loading, the maximum strains are obtained from a gage placed adjacent to the slab edge and as near as possible to the point of tangency of the footprint and the slab edge. Maximum edge strains are measured in a direction parallel to the edge of the slab. Normally, all strains are measured on the top side of the slab due to the greater convenience in locating the footprints with respect to the gages. Experience with corresponding gages placed on the top and on the bottom of the slab has indicated that compressive strains at the top surface were numerically equal, within the limit of experimental accuracy, to the tensile strains measured on the bottom surface of the slab.

Where ϵ_m is the maximum strain measured in the model, the following relationships may be used for converting strain to stress for circular loaded areas:

Interior Stress:

$$\sigma_m = \frac{E_m \epsilon_m}{1 - \mu_m} \quad (4)$$

Edge Stress:

$$\sigma_m = E_m \epsilon_m \quad (5)$$

For purpose of illustration, let it be required to design a model for the following prototype condition where:

- $P = 50,000$ lbs. (single wheel)
- $p = 180$ psi inflation pressure
- $r = 9.40$ inches, defined as: $[P/\pi p]^{1/2}$
- $E = 4 \times 10^6$ psi
- $\mu = 0.20$
- $h = 14.0$ inches
- $l = 55.56$ inches

In addition, let it be required to evaluate the maximum interior stress beneath the loaded area.

Assuming that a model slab is constructed with $h_m = 0.1325$ inch, and on the basis of the

known values of E_m and μ_m for the Hydrostone, we obtain a value of $l_m = 2.0499$ inches. The length scale ratio, n , of the prototype to the model then becomes:

$$n = \frac{l}{l_m} = \frac{55.56}{2.0499} = 27.104$$

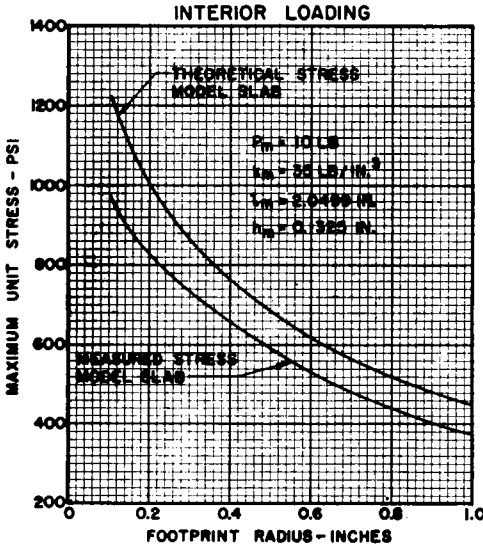


Figure 2. Comparison of measured and theoretical maximum stresses for a circular load in the interior of the slab.

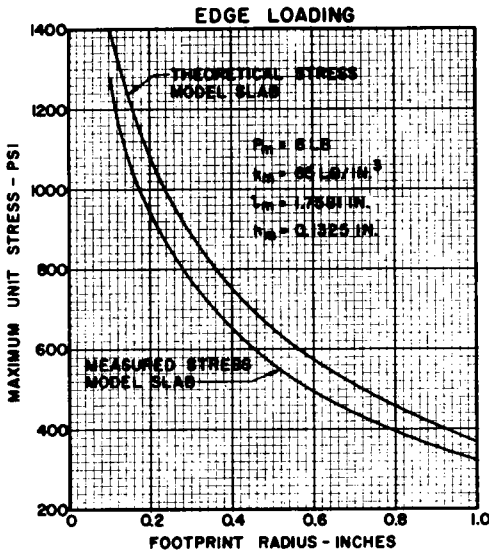


Figure 3. Comparison of measured and theoretical maximum stresses for a circular load tangent to a free edge.

This ratio n is used for establishing the radius of the loaded area, r_m , for the model (from Equation 1), and also may be used for dimensioning major and minor axes for simulating elliptical loaded areas, as well as dimensioning wheel gear configurations on the model. For the case of the circular loaded area set up in the example, then:

$$r_m = \frac{r}{n} = \frac{9.40}{27.104} = 0.347 \text{ inch}$$

Selecting $P_m = 10$ lbs, the maximum interior strain is measured and converted to stress by Equation 4. Assuming that the selected values result in $\sigma_m = 698$ psi, the equivalent maximum stress, σ , in the prototype may be computed by substituting the known values of σ_m , μ_m , P_m , h_m , μ , P , and h in Equation 2. Using the values chosen for this illustration, $\sigma = 375$ psi.

A similar procedure is used for evaluating edge stresses, for circular loaded areas, employing Equations 3 and 5.

DISCUSSION OF MODEL ANALOGY

Maximum model stresses measured for both interior and edge loading, and for a wide range of footprint radii are shown in Figures 2 and 3. Also shown in these figures are the theoretical maximum model stresses based on Westergaard's equations for interior and edge loading. There is reasonably good correlation between the maximum stresses measured in the model and those stresses based on the Westergaard theoretical analysis. Much of the differences shown in Figures 2 and 3 may be due to a combination of the model not meeting precisely the assumptions of the theory and to the evaluation of the physical constants of the model materials. It is also possible that some error is introduced due to the finite length of the strain gage, although a reduction in the gage length from 0.25 inch to 0.07 inch does not produce any significant changes in the maximum measured strains. It is particularly

encouraging to note that the model follows the Westergaard theory especially well in denoting relative changes in stress resulting from a change in the condition of loading.

When model measurements are compared with those obtained from full scale or prototype tests, such as described in Reference 3, the model stresses are somewhat higher and fall between the stresses measured in the prototype tests and those indicated by the theory. In all cases, however, the relative distribution of stress is in good agreement.

Although no data are presented in this paper, a limited amount of study has been made relative to the correlation of Pickett's Elastic Solid Theory with the model. Based on the assumption that the supporting medium acts as an elastic solid of semi-infinite extent, equally good correlation was obtained for the condition of interior loading. For the case of edge loading, however, the correlation of measured stresses with theoretical stresses based on Pickett's theory was not encouraging. It is believed that the reasons for this apparent lack of correlation are the physical limitations in the model and the limited conditions for which the present solution of the theory applies.

The chief value of this type of model lies in the fact that it is essentially an analog device. In this sense it becomes a valuable tool for studying, on a qualitative basis, a large range of prototype conditions. Two examples of this type of analysis follow: (1) a study of the effect of high contact pressures, and (2) the effect of selected multiple wheel loadings.

EFFECT OF HIGH CONTACT PRESSURE

The model results presented in Figures 2 and 3 were developed in connection with a study of the effect of high tire inflation or contact pressures on concrete airfield pavement requirements. At the present time, contact pressures for military aircraft range from 40 to 200 psi. Maximum tire inflation pressures have increased from 100 psi to 200 psi over the past 4 or 5 years and there is every indication that tire pressures will continue to increase. The effect of an increase in tire inflation pressure on rigid pavement thickness requirements is shown in Figure 4 for a specific case of a pavement having a flexural strength of 700 psi and supported by a subgrade whose modulus is 100 pounds per cubic inch. The three loadings

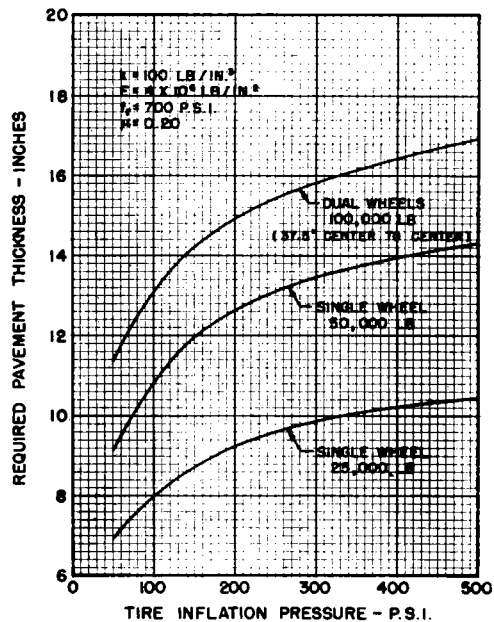


Figure 4. Effect of tire inflation pressure on the required thickness of pavement for three selected gear loadings & configurations. (Edge loading, Model results)

shown are: (1) a 25,000-pound single wheel load, (2) a 50,000-pound single wheel load, and (3) a 100,000-pound dual wheel load with the wheels spaced on 37.5-inch centers. The first and last loadings represent the present light and heavy duty pavement requirements of the Air Force, with tire pressures in each case being about 200 psi. These results were obtained directly from Figure 3 by the method of conversion outlined in the preceding portion of the paper. For this reason, the results presented in Figure 4 are necessarily limited to an equivalent circular loaded area rather than the elliptical shape usually assumed for an actual tire contact area. In addition, the curve for the 100,000-pound dual wheel load is based on the assumption that for 37.5-inch center to center spacing of the wheels, the maximum stress induced by the combined wheels would be equal to the maximum stress produced by a single wheel having the same contact area and loaded to 75,000 pounds. The validity of this latter assumption is shown in the succeeding section of this paper which describes the effect of multiple wheel loadings.

From the curves shown in Figure 4, it can

be seen that the required increase in pavement thickness due to an increase in tire inflation pressure from 200 to 500 psi only slightly exceeds the increase in thickness required in raising tire inflation pressures from 100 to 200 psi. Experience obtained through full scale traffic tests indicates that the relative requirements for 100 and 200 psi inflation pressures are reasonably accurate. Comparison of the required pavement thicknesses shown by these curves with the required thicknesses indicated by design curves now in use show that the values indicated by the model are within 1 inch of our normal design requirements for inflation pressures up to 200 psi. At the present time, no experience records are available to show the effect of contact pressures greater than 200 psi on the design requirements for concrete pavements.

EFFECT OF MULTIPLE WHEEL LOADING

General:—The method of model analysis described in the preceding portions of this paper is being applied to a study of multiple wheel loading. The use of multiple wheel gear assemblies for heavy cargo and bomber-type military aircraft has become a common practice of the aircraft designer, with maximum gross aircraft weights approaching and exceed-

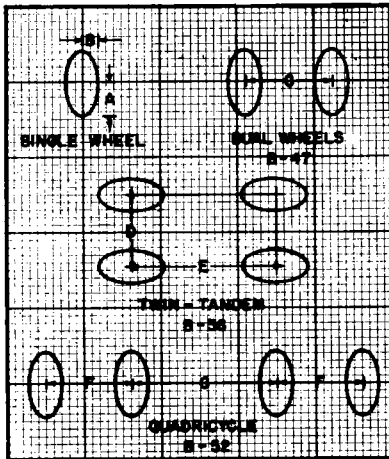
ing 400,000 pounds. Three aircraft of the heavy bomber type, the B-47, the B-36, and the B-52 use dual, twin-tandem, and quadricycle gear, respectively. The tire size is the same for all planes, and in the actual operation of the aircraft the tire pressures are controlled by keeping the deflection of the tires constant. This limitation in the deflection automatically provides a constant tire contact area for all tires used in the main gear of these aircraft, regardless of the gross operational weights of the planes. Consequently, by using equal and constant contact areas for theoretical and model analyses, the procedure is simplified and the scope of application made a maximum.

In these analyses, the load is assumed to be distributed uniformly over the elliptically shaped contact area of the individual tire. Although this is not necessarily true for either the model or the prototype, the effect of this discrepancy on the maximum stress along the base of a rigid pavement slab is negligible.

Model Design and Testing:—The three typical gear configurations used in these studies are shown in Figure 5, with the appropriate model and prototype dimensions. The length scale ratio of the prototype to the model was kept constant at 40:1 throughout the tests. Three different values of l_m were studied in the model analysis, l_m being varied by using three different thicknesses of model slabs and maintaining all other properties constant.

The critical positioning of each gear configuration on the pavement slab was investigated for both interior and edge loading. In loading the model slab, simulation of the multiple wheel configurations was accomplished by placing the single wheel footprint successively in each of the relative prototype wheel positions, making separate strain measurements for each position of the footprint, and adding algebraically by the method of superposition the individual strains to obtain the maximum strain for each gear. All tests were made using the single wheel footprint and the resulting multiple wheel data related to an equivalent single wheel having an identical tire contact area.

Results:—For interior loading, the position of the maximum stress is dependent upon the gear configuration. In all cases, the maximum stress occurs directly under the center of one of the contact areas. For symmetrical configurations such as the dual wheel and twin-tandem gear, the maximum stress for each



| DIMENSION | A | B | C | D | E | F | G |
|-----------|------|------|------|------|------|------|------|
| MODEL | 0.30 | 0.10 | 0.93 | 0.78 | 1.56 | 0.93 | 1.56 |
| PROTOTYPE | 11.9 | 7.14 | 37.5 | 31 | 62 | 37.5 | 62 |

NOTE: ALL DIMENSIONS ARE IN INCHES
ALL CONTACT AREAS ARE EQUAL

Figure 5. Model and Prototype gear dimensions used in the multiple wheel study.

TABLE 1

COMPARISON OF MAXIMUM MEASURED & THEORETICAL STRESSES FOR SINGLE WHEEL, DUAL WHEEL, TWIN-TANDEM AND QUADRICYCLE GEAR CONFIGURATIONS - EDGE LOADING.

| CRITICAL ORIENTATION OF GEAR | MAXIMUM STRESS P.S.I. | | PERCENT OF TOTAL STRESS CONTRIBUTED BY EACH WHEEL | | | |
|---|-----------------------|------|---|-----------------------------|-----------------------------|--|
| | MEAS | THEO | WHEEL | MEAS | THEO | |
| SINGLE WHEEL  | 939 | 1031 | I | 100.0 | 100.0 | |
| DUAL WHEEL  | 1260 | 1409 | I II | 74.5 25.5 | 73.2 26.8 | |
| TWIN-TANDEM  | 1368 | 1627 | I II III IV | 62.5 15.8 12.5 9.2 | 59.2 18.0 13.1 9.7 | |
| QUADRICYCLE  | 1410 | 1584 | I II III IV | 66.6 22.8 7.0 3.6 | 65.2 23.8 7.0 4.0 | |

- NOTES:
- THESE RELATIONSHIPS ARE FOR THE FOLLOWING CONDITIONS:
 - EQUAL LOADS ON ALL WHEELS ($P_m = 6 \text{ LB}$)
 - CONSTANT CONTACT AREA.
 - RADIUS OF RELATIVE STIFFNESS, $l_m = 1.7626 \text{ IN.}$
 - $h_m = 0.133 \text{ IN.}$; $k_m = 65 \text{ LB/IN.}^3$
 - → SHOWS POSITION AND DIRECTION OF MAXIMUM STRESS.

gear occurs under each wheel. For the quadricycle gear, however, the maximum stress occurs only under the two interior wheels. For edge loading, the maximum stress occurs at and parallel to the edge, with the most critical positioning of the wheel assemblies being as shown in Table 1. This Table also shows a comparison of maximum measured and theoretical stresses for the single and multiple wheel assemblies. In all cases, the model stresses are less than those indicated by the theory, with the relative differences being similar to those noted in the high contact pressure study. However, as can be seen in the last two columns of Table 1, the agreement between the measured and theoretical values is excellent relative to the percent of total stress contributed by each wheel. Another interesting comparison of data obtained from the model is the ratio of the critical edge stress to the critical interior stress for similar conditions of loading. A summary of these data for both measured and theoretical stresses is presented in Table 2. Here again, remarkably good agreement between model and theoretical values is indicated.

The results of edge loading tests for these studies are consolidated in Figure 6. These curves show the effect of the radius of relative stiffness, l , on the ratio of the total gear load to a single wheel load producing the same

TABLE 2
RATIO OF MAXIMUM STRESSES FOR EDGE AND INTERIOR LOADING

| Wheel Assembly | Measured* | | Theoretical* | |
|------------------|--------------------------------------|--------------------------------------|--------------------------------------|--------------------------------------|
| | Edge σ_m /Interior σ_m |
| Single..... | 1.94 | | 1.77 | |
| Dual..... | 1.83 | | 1.83 | |
| Twin-Tandem..... | 1.56 | | 1.61 | |
| Quadricycle..... | 1.55 | | 1.56 | |

* Limited to equal loads on all wheels and constant contact areas.

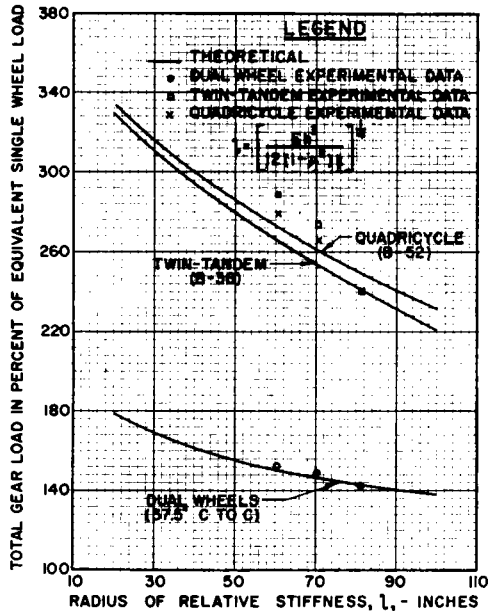


Figure 6. Effect of l on the ratio of the total load to the equivalent single wheel load for contact areas of 267 sq. in. for all wheels.

maximum stress. The solid lines give the theoretical relationship, while the plotted points are experimental data for the three values of l_m translated to prototype values. The points determined experimentally for the twin-tandem gear for l in the range of 60 and 70 inches appear out of line with the theory, otherwise the agreement between experimental and theoretical data is good. It should be pointed out that in computing the total gear loads in terms of percent of the equivalent single wheel load, any experimental error is magnified by a factor equal to the number of wheels comprising the gear.

Application:—The curves presented in Figure 6 are of considerable value in both the design and evaluation of rigid pavements, for it

TABLE 3
EFFECT OF MULTIPLE WHEEL GEAR ON PAVEMENT LOAD CARRYING CAPACITY

| Wheel Assembly | Percent Increase* Over Equivalent Single Wheel | Gear Load Lbs. | Gross Weight of Aircraft Lbs. |
|-------------------------|--|----------------|-------------------------------|
| Single..... | 0 | 67,000 | 149,000 |
| Dual (B-47)..... | 150 | 100,500 | 182,500 |
| Twin-Tandem (B-36)..... | 266 | 178,000 | 395,500 |
| Quadricycle (B-52)..... | 273 | 182,000 | 332,500 |

* Obtained from Figures 6 for $l = 60$ inches.

can be seen that there is little difference in the design requirements for equivalent twin-tandem and quadricycle gear loadings; and that there is an appreciable advantage obtained in the load carrying capacity of a pavement when a four-wheel assembly is used instead of a single wheel or a dual wheel assembly. For example, the values given in Table 3 show what these curves mean in pavement capacity for a 16-inch pavement with a radius of relative stiffness, l , of 60 inches and a capability of carrying a single wheel load of 67,000 pounds. Since the Corps of Engineers' rigid pavement design curves are based on critical edge stresses, the values in the above table are directly applicable to the evaluation of the pavement selected for the illustration.

SUMMARY AND CONCLUSIONS

The type of model described in this paper is an excellent analog device for studying a wide variety of problems arising in connection with concrete airfield pavement design and evaluation.

This model analogy, when applied to the study of high contact pressures and multiple wheel gear, can be correlated with the theoretical solutions for similar conditions of loading.

This method of analysis can be used for studying conditions for which specific theoretical solutions have not been developed or where there is some doubt as to their applicability; i.e., it can be used as a basis for evaluating new theories and extending the usefulness of those already developed.

In the case of the effect of high contact pressure given in this paper, it is shown that on the basis of both the model and the theoretical analysis, for an increase in tire inflation

pressure from 200 psi to 500 psi, the required increase in pavement thickness will not be much greater than that required for an increase from 100 psi to 200 psi.

The analysis of the effect of distributing aircraft loads through the use of multiple wheel gear illustrates the possibility as well as the limitations which may be encountered in basing the design and evaluation of airfield pavements on a single equivalent wheel load having a constant contact area.

ACKNOWLEDGMENTS

The studies reported in this paper have been carried out by members of the Staff of the Ohio River Division Laboratories as a part of the Corps of Engineers, U. S. Army, Rigid Pavement Investigational Program. This program is directed and coordinated by members of the Airfields Branch, Engineering Division for Military Construction, Office, Chief of Engineers. This work was done under and by the authority of the Chief of Engineers, U. S. Army.

REFERENCES

1. ROBERT R. PHILIPPE, "Structural Behavior of Concrete Airfield Pavements—The Test Program". Vol. 24, 1944 Proceedings of the Highway Research Board.
2. ROBERT R. PHILIPPE, "Use of Reinforcement in Concrete Pavements". Vol. 28, 1948 Proceedings of the Highway Research Board.
3. ROBERT R. PHILIPPE AND CARL H. CHRISTIANSEN, "The Overlay of Rigid Pavements". Vol. 30, 1950 Proceedings of the Highway Research Board.
4. R. R. PHILIPPE AND F. M. MELLINGER, "Structural Behavior of Heavy Duty Concrete Airfield Pavements". Vol. 31, 1952 Proceedings of the Highway Research Board.
5. H. M. WESTERGAARD, "New Formulas for Stresses in Concrete Pavements of Airfields". Transactions, American Society of Civil Engineers, 1947, Vol. 113, Page 425.
6. G. PICKETT ET AL., "Deflections, Moments and Reactive Pressures for Concrete Pavements". Kansas State College Bulletin No. 65, Oct. 1951.